AD-A156 477 SUB-CLOUD LAYER MOTIONS FROM RADAR DATA USING CORRELATION TECHNIQUES. (U) SYSTEMS AND APPLIED SCIENCES CORP VIENNA VA G R SMYTHE ET AL. 15 OCT 84 SCIENTIFIC-5 AFGL-TR-84-0272 1/1

UNCLASSIFIED F/G 4/2 NL

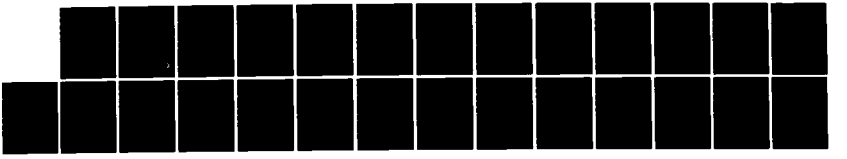

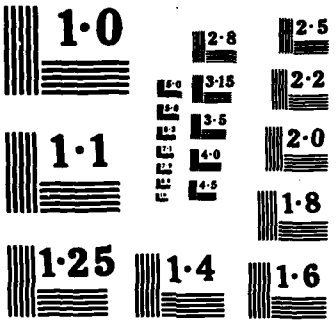

NATIONAL BUREAU OF STANDARDS
MICROCOPY RESOLUTION TEST CHART

AFGL-TR-84-0272

SUB-CLOUD LAYER MOTIONS FROM RADAR DATA USING CORRELATION TECHNIQUES

Glenn R. Smythe
F. Ian Harris

Systems and Applied Sciences Corporation (SASC)
1577 Springhill Road, Suite 600
Vienna, Virginia 22180

October 15, 1984

Scientific Report No. 5

AIR FORCE GEOPHYSICS LABORATORY
AIR FORCE SYSTEMS COMMAND
UNITED STATES AIR FORCE
HANSCOM AFB, MASSACHUSETTS 01731

This technical report has been reviewed and is approved for publication.

ALIAN J. BUSSEY
Contract Manager

Accession For	
NTIS GRA&I	X
DTIC TAB	☐
Unannounced	☐
Justification	
By	
Distribution/	
Availability Codes	
Dist	Avail and/or Special
A/1	

FOR THE COMMANDER

ROBERT A. McCLATCHEY, Director
Atmospheric Sciences Division

This report has been reviewed by the ESD Public Affairs Office (PA) and is releasable to the National Technical Information Service (NTIS).

Qualified requestors may obtain additional copies from the Defense Technical Information Center. All others should apply to the National Technical Information Service.

If your address has changed, or if you wish to be removed from the mailing list, or if the addressee is no longer employed by your organization, please notify AFGL/DAA, Hanscom AFB, MA 01731. This will assist us in maintaining a current mailing list.

UNCLASSIFIED

SECURITY CLASSIFICATION OF THIS PAGE

REPORT DOCUMENTATION PAGE

1a. REPORT SECURITY CLASSIFICATION UNCLASSIFIED	1b. RESTRICTIVE MARKINGS
2a. SECURITY CLASSIFICATION AUTHORITY	3. DISTRIBUTION/AVAILABILITY OF REPORT Approved for public release; distribution unlimited
2b. DECLASSIFICATION/DOWNGRADING SCHEDULE	
4. PERFORMING ORGANIZATION REPORT NUMBER(S)	5. MONITORING ORGANIZATION REPORT NUMBER(S) AFGL-TR-84-0272
6a. NAME OF PERFORMING ORGANIZATION Systems & Applied Sciences Corporation (SASC) 6b. OFFICE SYMBOL (If applicable)	7a. NAME OF MONITORING ORGANIZATION Air Force Geophysics Laboratory
6c. ADDRESS (City, State and ZIP Code) 1577 Springhill Rd, Suite 600 Vienna, VA 22180	7b. ADDRESS (City, State and ZIP Code) Hanscom AFB MA 01731 Manager/LY/Allan J. Bussey
8a. NAME OF FUNDING/SPONSORING ORGANIZATION Air Force Geophysics Laboratory 8b. OFFICE SYMBOL (If applicable) LY	9. PROCUREMENT INSTRUMENT IDENTIFICATION NUMBER Contract No. F19628-82-C-0023
8c. ADDRESS (City, State and ZIP Code) Hanscom AFB MA 01731	10. SOURCE OF FUNDING NOS. PROGRAM ELEMENT NO.: 62101F PROJECT NO.: 6670 TASK NO.: 00 WORK UNIT NO.: AC
11. TITLE (Include Security Classification) Sub-Cloud Layer Motions from Radar Data Using Correlation Techniques	
12. PERSONAL AUTHOR(S) Glenn R. Smythe and F. Ian Harris	
13a. TYPE OF REPORT Scientific Rpt. No. 5 13b. TIME COVERED FROM _____ TO _____	14. DATE OF REPORT (Yr., Mo., Day) 84/10/15 15. PAGE COUNT 24
16. SUPPLEMENTARY NOTATION	

17. COSATI CODES			18. SUBJECT TERMS (Continue on reverse if necessary and identify by block number)
FIELD	GROUP	SUB. GR.	Weather radar; Doppler weather radar; Correlation techniques; Pattern recognition; Pattern tracking; NEXRAD
0401			
0402			

19. ABSTRACT (Continue on reverse if necessary and identify by block number)

Acquisition of a new system of Doppler weather radars (NEXRAD, Next Generation Weather Radar) will necessitate availability of appropriate automated weather analysis algorithms. In this report one such algorithm for obtaining small-scale motions from radar data by pattern recognition is evaluated. Two variations that correlate reflectivity data from scan to scan, one of which utilizes Doppler velocities, are applied to data of two intense thunderstorms. From these analyses it is found that resolution typical of most weather radars is too coarse to allow consistently reliable reconstruction of motions with temporal lags short enough to preclude discernible effects of propagation.

20. DISTRIBUTION/AVAILABILITY OF ABSTRACT UNCLASSIFIED/UNLIMITED ☒ SAME AS RPT. ☐ DTIC USERS ☐	21. ABSTRACT SECURITY CLASSIFICATION UNCLASSIFIED
22a. NAME OF RESPONSIBLE INDIVIDUAL Allan J. Bussey	22b. TELEPHONE NUMBER (Include Area Code) (617) 861-2977 22c. OFFICE SYMBOL LY

DD FORM 1473, 83 APR EDITION OF 1 JAN 73 IS OBSOLETE.

UNCLASSIFIED

SECURITY CLASSIFICATION OF THIS PAGE

TABLE OF CONTENTS

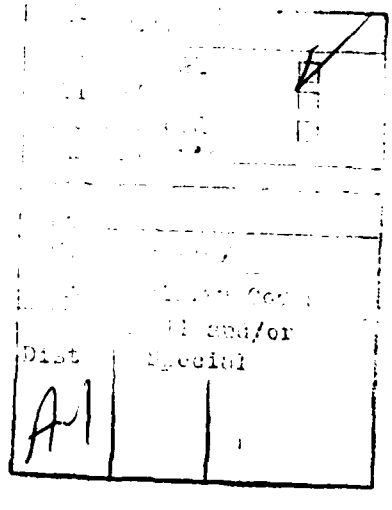

I. INTRODUCTION

The Next Generation Weather Radar (NEXRAD) program is a joint project of the U.S. Departments of Defense, Transportation, and Commerce. Its purpose is to develop a new national network of weather radars to replace the antiquated system currently in use. With this new technology there arises a need for automated radar data analysis schemes that will extract pertinent information (i.e., indicators of hazardous weather conditions) from the data and provide it to the operations meteorologist in a useful form. A primary requirement is the accurate estimation of low level winds, particularly those associated with gust fronts and downbursts. The standard wind estimation techniques developed for Doppler radar yield only large-scale estimates (on the order of 10^3 km^2) and, hence, do not lend themselves to hazard detection. This paper evaluates an alternative wind estimation technique for extracting small-scale motion, currently under consideration for the NEXRAD program.

Rinehart [1979][1] and Smythe and Zrnic' [1983][2] each proposed a variation of a correlation-pattern-recognition technique for extracting small-scale atmospheric motions (~5-15 km) from single station non-Doppler (Rinehart) and Doppler (Smythe and Zrnic') radar data. Small region (boxes) of reflectivity data from one radar scan are correlated with equally dimensioned regions of data from a later scan at the same elevation. A box from one scan is lagged radially and azimuthally within a specified search area of a later scan in order to identify the pattern that correlates best. Both use the standard correlation coefficient equation and compute pattern motions from the spatial displacement between pattern locations divided by temporal lag.

---

1. Rinehart, R. E., 1979: Internal Storm Motions from a Single Non-Doppler Weather Radar. NCAR/TR-146+STR, National Center for Atmospheric Research, Boulder, CO, 262 pp.

2. Smythe, G. R., and D. S. Zrnic', 1983: Correlation analysis of Doppler radar data and retrieval of the horizontal wind. J. Clim. Appl. Meteor., 22, 297-311.

The Rinehart and Smythe and Zrnic' variations differ mainly in the way the search area is determined. Our interpretation of and modifications to their schemes are as follows: Variation V1 (similar to Rinehart) sets up a circular area (Fig. 1) with radius equal to the product of a subjectively determined maximum velocity (V_{max}) and the elapsed time between the two scans (Δt). When Doppler information is available, then variation V2 (similar to Smythe and Zrnic') may be used (see Fig. 1). In V2 Doppler velocities averaged over the initial box ($\bar{V}$) are used to estimate the radial displacement ($d = \bar{V}.\Delta t$) of the pattern. The standard deviation of the radial velocities σ_V is incorporated to allow for small adjustments ($\Delta d = \sigma_V . \Delta t$) to d, thereby giving the radial dimension of the search area ($D = \pm k . \Delta d$, where k is a pre-determined constant). It is assumed that the pattern moves with the local mean air motion. One advantage to using V2 is that the search area is reduced considerably, lessening computer processing time. V2 documentation is contained in the Appendix.

In this report we attempt to extract motions in the sub-cloud layers of two intense storms. Both V1 and V2 are applied to data from a storm that occurred on April 10, 1979 southwest of Norman, OK and results are compared. The second storm occurred on June 22, 1976 near Grover, CO. Since no Doppler data with the necessary temporal and spatial resolution were available, only V1 is applied in the Colorado case. Results are compared with winds synthesized from data of three Doppler radars that scanned the Grover area.

II. OKLAHOMA THUNDERSTORM OF APRIL 10, 1979 - A DOPPLER CASE

Between 1700 and 1800 CST the National Severe Storms Laboratory (NSSL) 10 cm Doppler radar collected data in sector scans at 0.5° elevation in one-minute intervals. The data resolution is 1° and 600 m for reflectivity and 150 m for velocity (maximum ranges of 460 and 115 km, respectively). Velocities are unfolded with respect to range and Nyquist velocity, and averaged radially over four gates. Reflectivities are thresholded at 10 dBZ. Fig. 2 shows the reflectivity field at 1715, the beginning time for the correlation analysis. Unfortunately there are no dual-Doppler airflow fields available to compare with the motion fields. Instead, the fields obtained from V1 and V2 are compared to test for

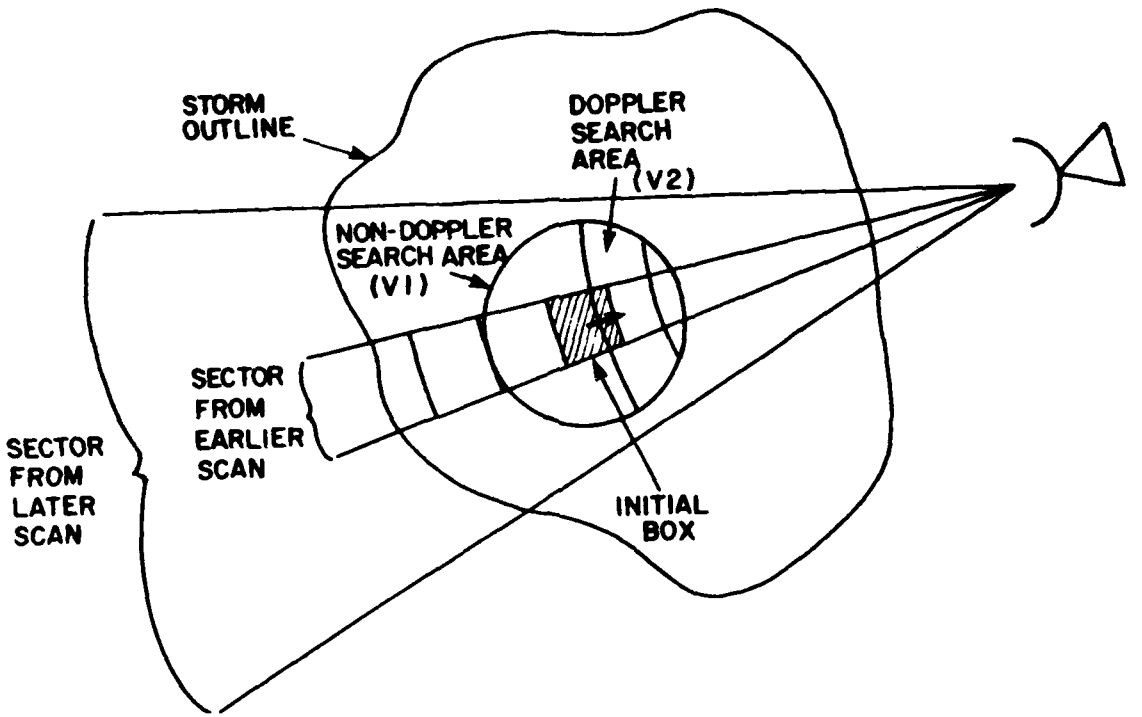

Fig. 1. Geometry of Search Areas Used for Correlation Analyses

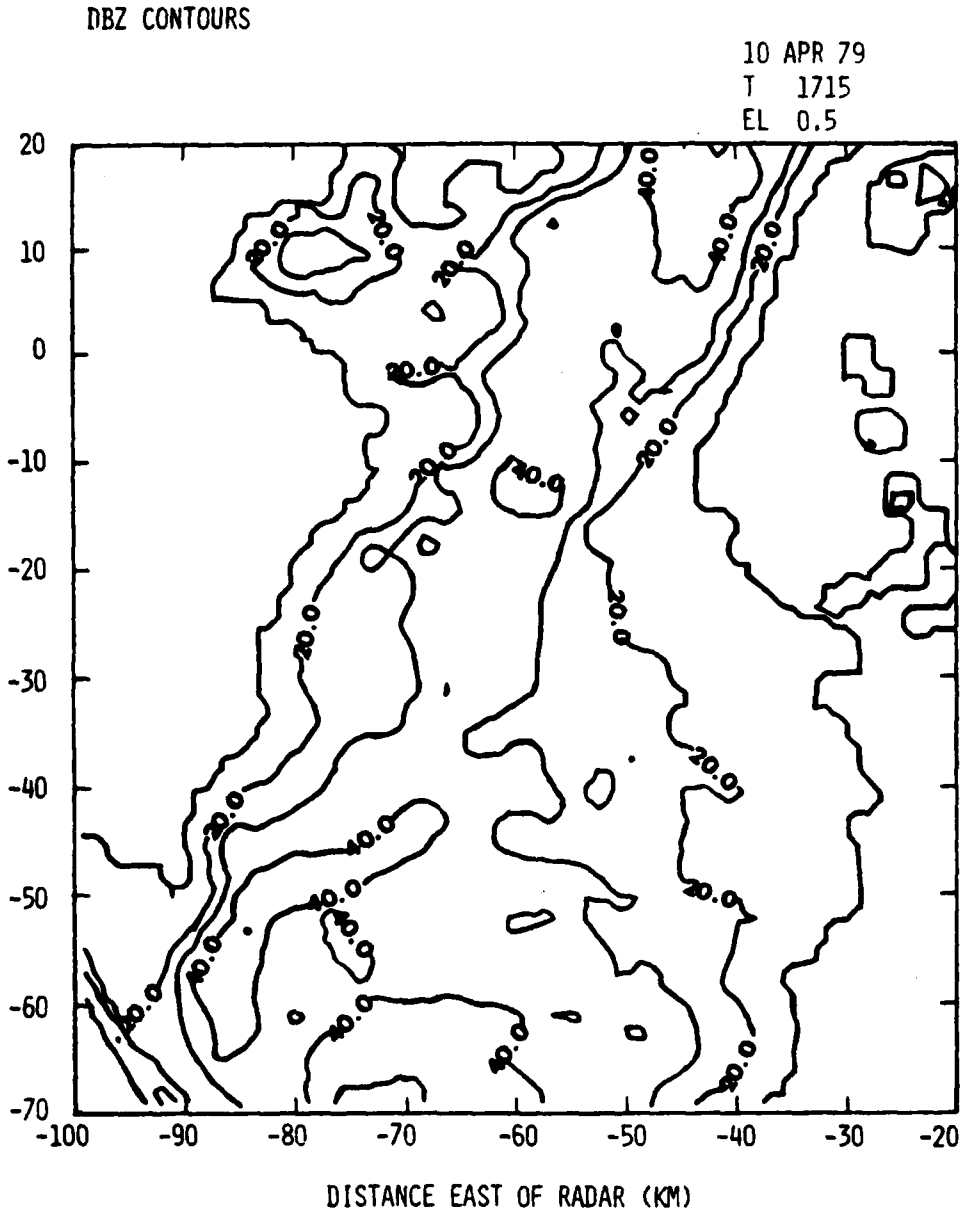

Fig. 2. Reflectivity Contours in dBZ from Scan 1715, April 10, 1979

consistency and then the case in Section III (Colorado) is used for verification of the overall technique.

V2 was applied to several scans using a search area with k = 4 and Δt = 66 s. The result from one such analysis is shown in Fig. 3. Fig. 4 depicts the motion field obtained by applying V1 to the same data. In both cases V_{max} = 40 m . s^{-1} and the box size is 6 km x 4°. With the exception of the radial vectors (to be discussed in Section IV) in the west to southwest the flow is, in general, southerly. There are few differences in the two fields; however, from examination of the correlation fields, it was found that in some cases (e.g., at (-57 East, -67 North) km and (-52, -47) km in Fig. 3) use of Doppler information with V2 underestimates the search areas and hence the radial lag of maximum correlation. There are two possible reasons for this: either the mean radial velocity was not a reasonable estimate of the motion of the feature or the variability of the radial velocities was insufficient to allow Δd to be large enough to include the maximum correlation. The degree of consistency in Figs. 3 and 4 was seen for all motion fields derived from scans 66 s apart between 1715 and 1723 (not shown). It should be noted that the processing time for V2 was less than 50 percent of that for the conventional radar (V1).

III. COLORADO THUNDERSTORM OF June 22, 1976 - A NON-DOPPLER CASE

The eastern Colorado thunderstorm of June 22, 1976 was observed by National Center for Atmospheric Research (NCAR) staff during the National Hail Research Experiment with the aid of one non-Doppler (CP-2) and four Doppler radars [Knight and Squires, ed., 1982].[3] CP-2 data were sampled every 0.5° in azimuth and 150 m in range and updated about every 2.5 min.

Fig. 5 depicts the reflectivity data for 1627 MDT. This storm appears to have more structure than that depicted in Fig. 2. This structure should facilitate use of the correlation techniques. Fig. 6 results from applying V1 to scans at 1627 and 1629 with V_{max} = 40 m . s^{-1} and a box size of 6 km x 4°. There is consistency with analyses of successive scans at 1.2° (1627 through 1632) and with analyses at 0.5° elevation (not

3. Knight, C.A., and P. Squires, ed., 1982: Hailstorms of the Central High Plains, II: Case Studies of the National Hail Research Experiment. National Center for Atmospheric Research, Boulder, CO, 245 pp.

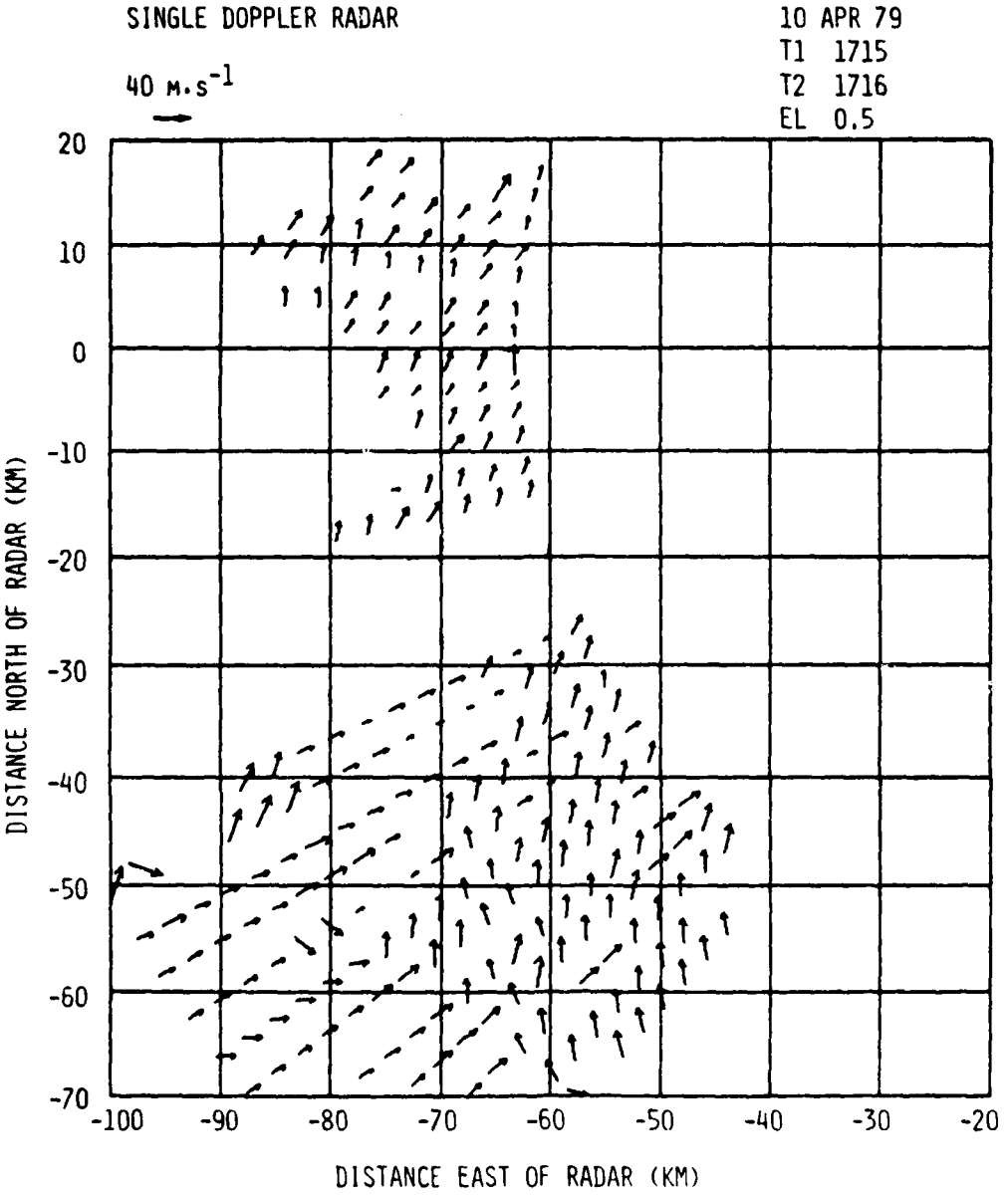

Fig. 3. Motions from April 10, 1979 Oklahoma Thunderstorm Obtained Using Averaged Doppler Velocities to Estimate Radial Displacement of Weather Targets (V2)

(Scan times are 1715 and 1716 with a 66 s lag; elevation angle is 0.5°; box dimensions are 6 km x 4°.)

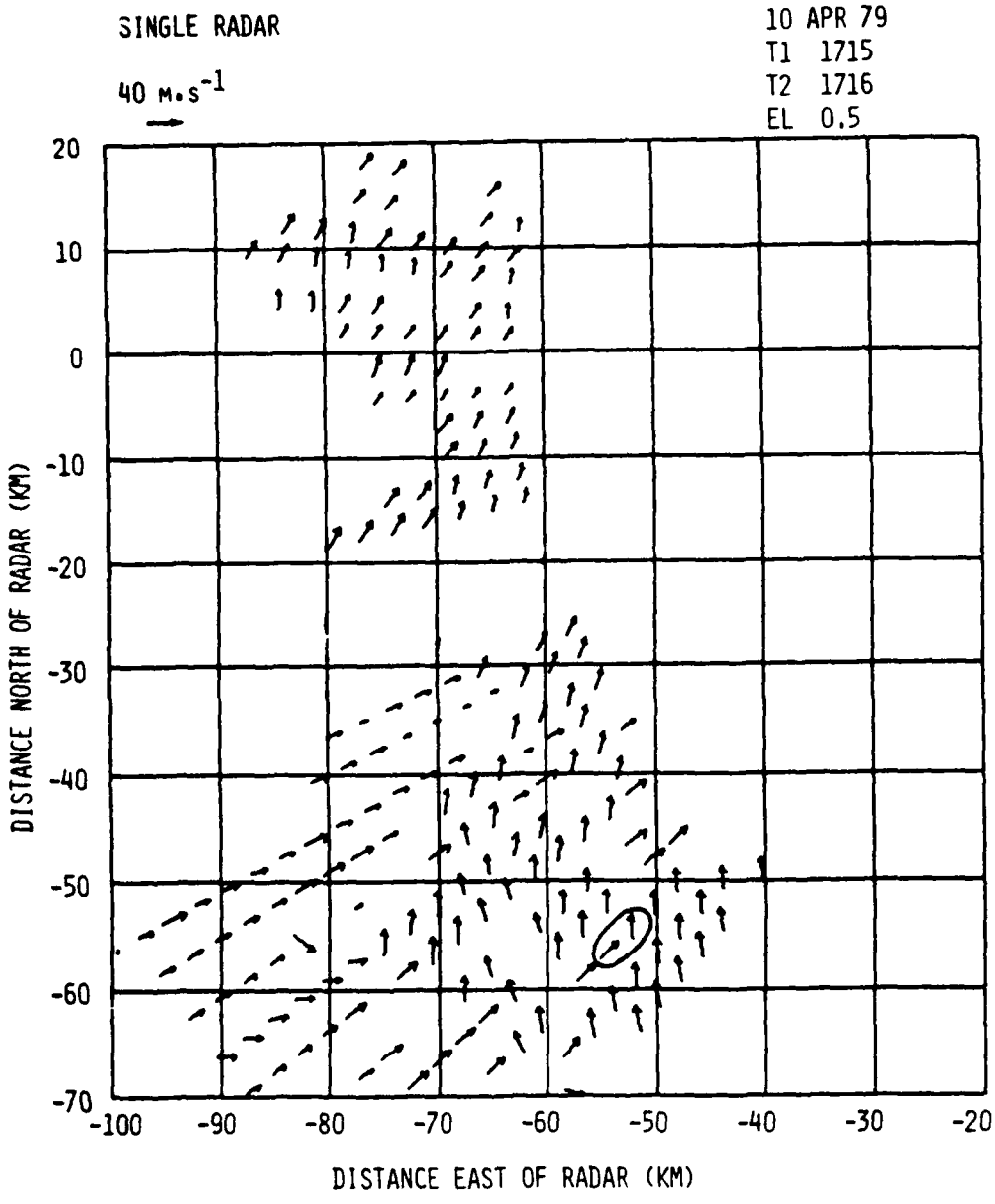

Fig. 4. As in Fig. 3, Except Single-Radar Motions Were Obtained Without Doppler Information (V1)

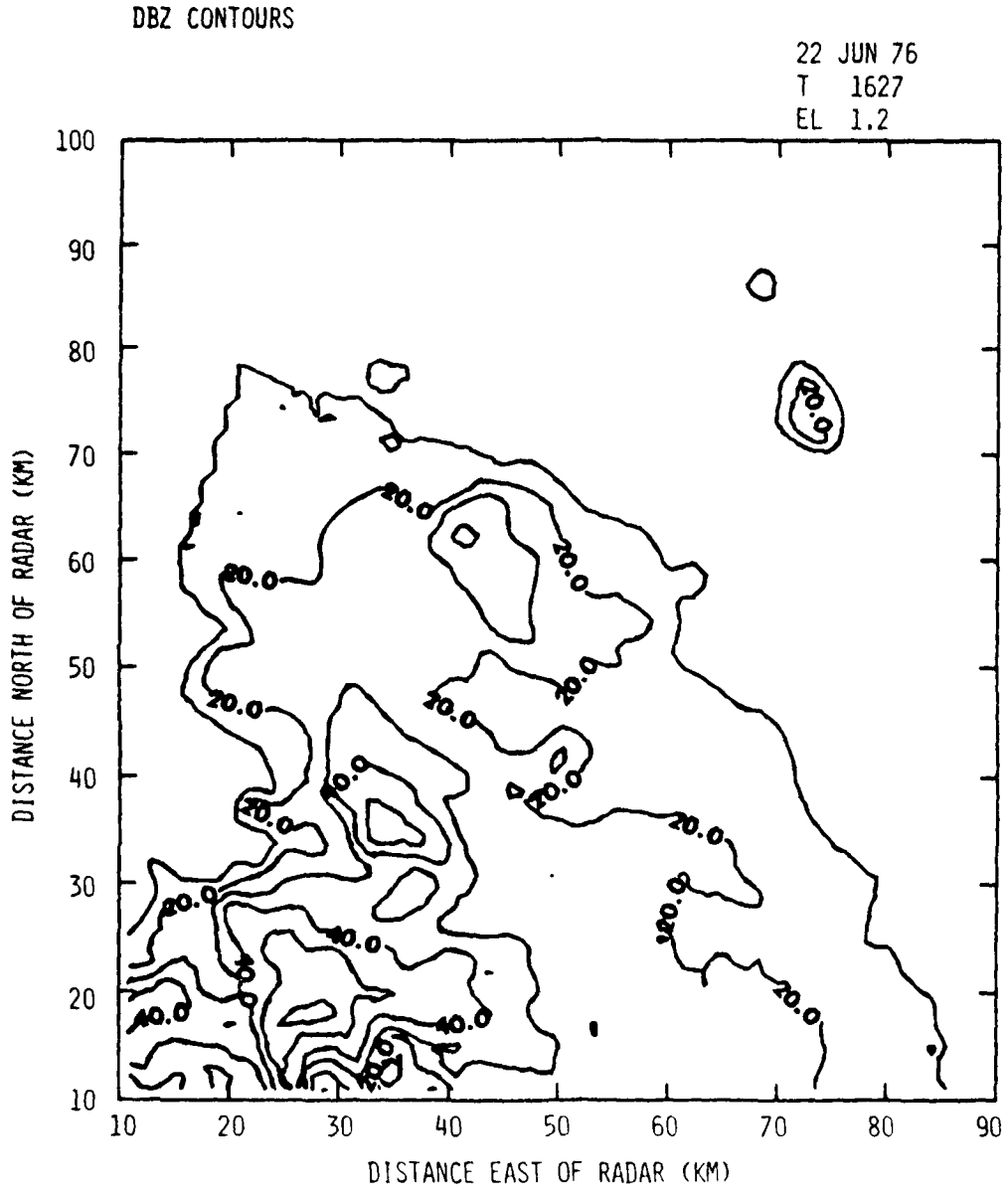

Fig. 5. Reflectivity Contours in dBZ from Scan 1627, June 22, 1976

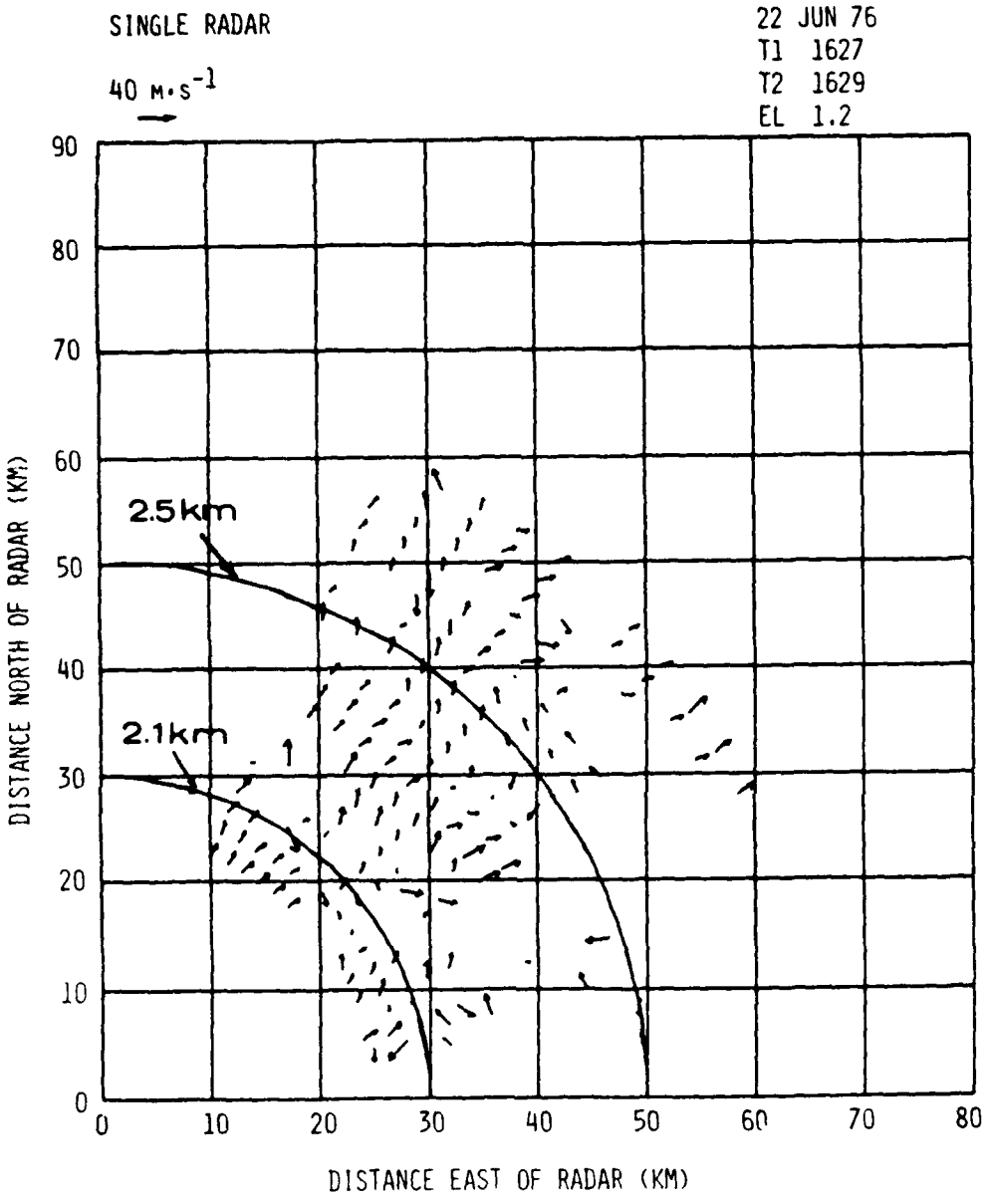

Fig. 6. Motions in June 22, 1976 *Colorado Thunderstorm* from Scans at 1.2° Elevation and Times 1627 and 1629

(Arcs represent heights (MSL) of data collection at ranges of 30 and 60 km.)

shown). Also the analysis presented in Rinehart and Garvey [1978],[4] although at 3.3° elevation, is quite similar to that in Fig. 6. An additional check was performed by manually following distinctive features in time. It was found that the correlation fields are in agreement with these manually derived fields, thus verifying that the algorithm is performing as designed.

Figs. 7 and 8 depict triple-Doppler radar airflow at 2 and 4 km above mean sea level (MSL) from the same volume scan (1625-1630) that corresponds to Fig. 6. Most of the single radar motions at heights from 2 to 2.5 km have southerly components but the airflow at 2 km has a predominantly northerly component. In fact, at some locations the motions are nearly 180° different from the airflow at 2 km. However, the airflow at 4 km does have a southerly component and is therefore in better agreement with the single radar motions. In addition here and in the analysis of Rinehart and Garvey [1978] for the same data, radial flow is again evident as in the Oklahoma case (Figs. 3 and 4).

IV. EFFECTS OF DATA RESOLUTION AND PROPAGATION

It is obvious from the preceding discussion that there are problems with the use of correlation techniques in the determination of wind fields on a routine and automatic basis. The main sources for these difficulties are the interrelationship between the temporal and spatial resolution of the data and the temporal and spatial scales of the patterns being tracked and the relative importance of propagation versus advection. To illustrate these points we will re-examine the discrepancies previously noted.

First we discuss errors due to inadequate spatial resolution. The vectors that are oriented radially in Figs. 3, 4, and 6 were produced because radial motions were too small to allow detection with 1° data resolution and Δt = 66 s. To illustrate this problem, a motion field produced by V1 with scans 132 s apart is shown in Fig. 9. There are fewer radial vectors than in Fig. 4 because with Δt = 132 s the patterns moved far enough for radial motion to be detected. At 100 km range and with 1°

4. Rinehart, R. E., and E. T. Garvey, 1978: Three-dimensional storm motion by conventional weather radar. Nature, 273, 287-289.

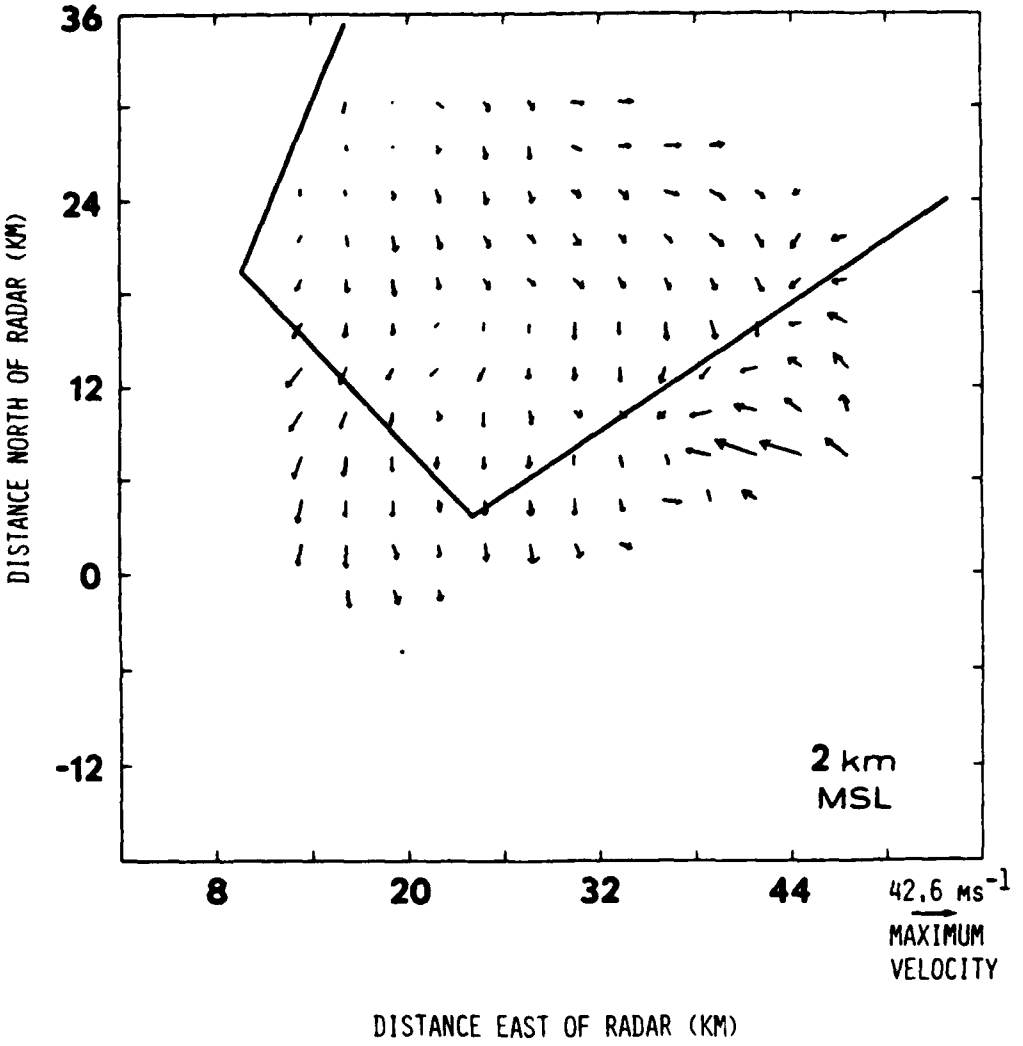

Fig. 7. Triple-Doppler Radar Airflow at 2km MSL from June 22, 1976 Volume Scan at 1625 - 1630

(Single-radar analysis region of Fig. 6 is outlined. Data were obtained through the courtesy of Mr. L. J. Miller of NCAR.)

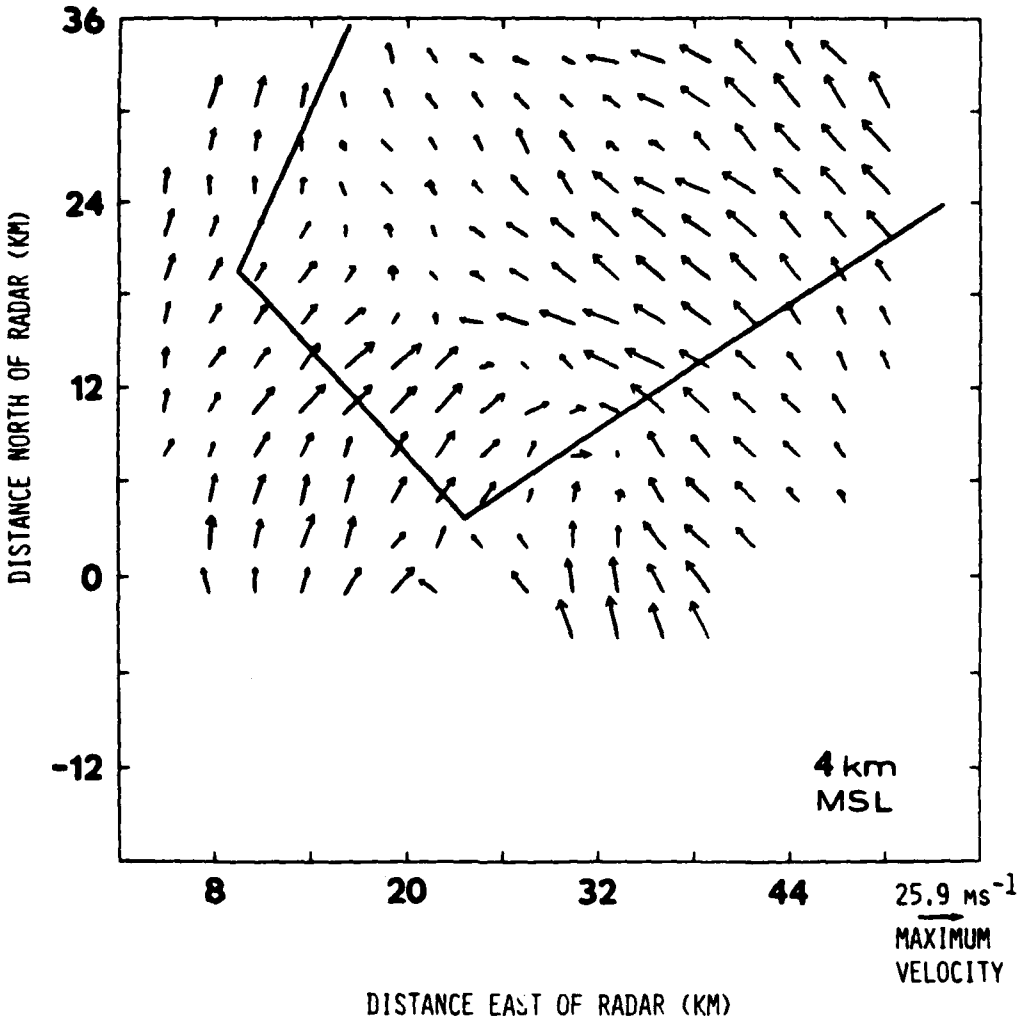

Fig. 8. As in Fig. 7, Except 4 km MSL

(Note arrow lengths are scaled differently than in Fig. 7.)

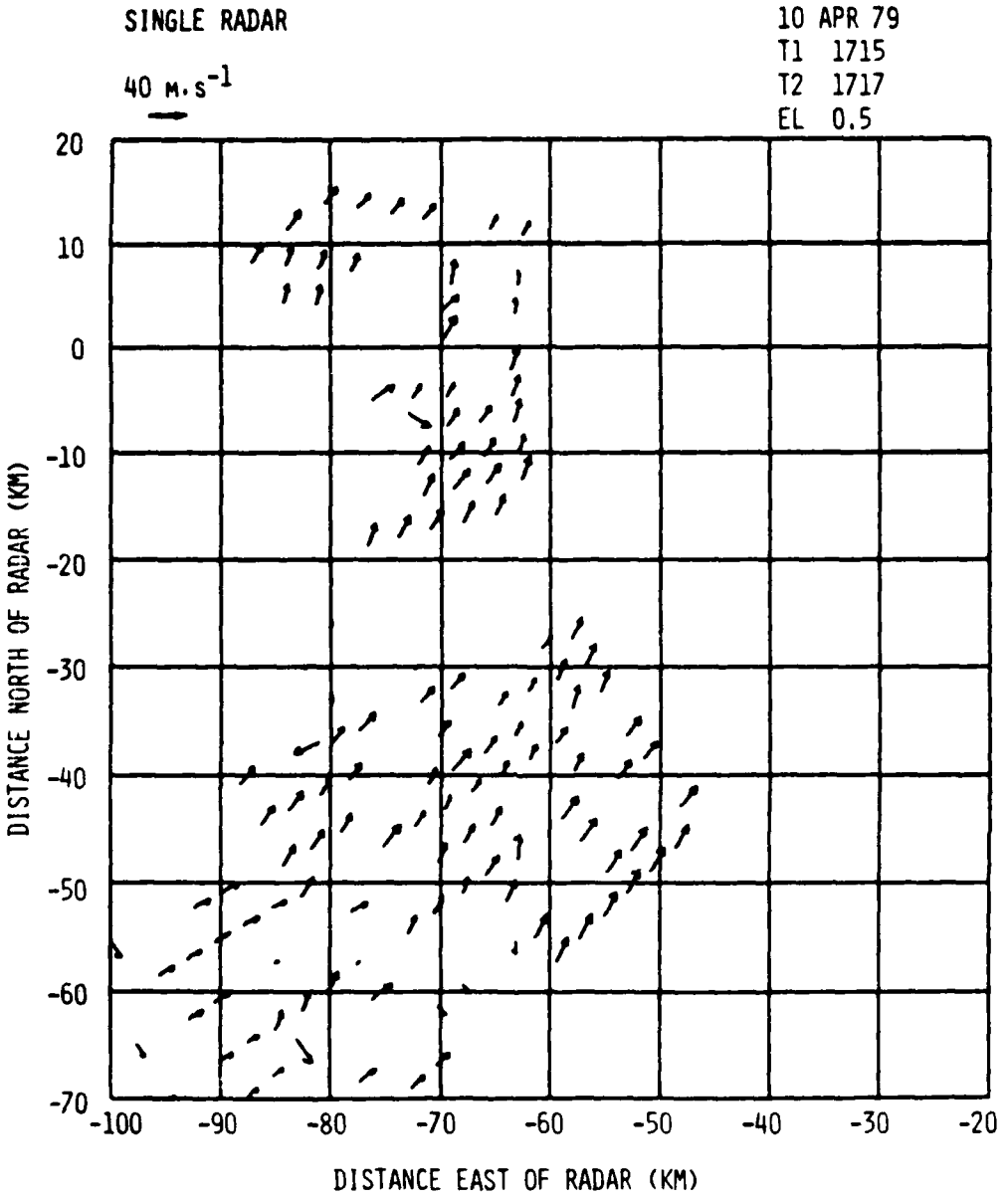

Fig. 9. As in Fig. 4, Except Temporal Lag is Increased from 66 s to 132 s and Scan Times are 1715 and 1717

resolution, patterns must travel 1.7 km azimuthally to be displaced by one radial. To realize this displacement in Δt = 66 s a speed of 26 m . s^{-1} is required.

A related error is exemplified by the vectors circled in Fig. 4. The one on the left is radial while the other has an azimuthal component of one lag (1°). In this case there is a potential error of 15° in direction alone with 1° resolution at a range of 77 km. Moreover, this error could be substantially greater if radial motion is much less than one lag. Interpolation between lag data points as performed in Rinehart [1979] might alleviate some of these resolution problems, but it may also produce fabricated motions if the correlation fields do not fit the interpolation model. For example, consider the field of squares of correlation coefficients shown as a function of beam lag (deg) and radial lag (number of gates) in Fig. 10. This field is the result of correlating one 6 km x 4° box with data from the next scan. Note the broad, flat region of high values between beam lags -5 and 0 and radial lags -1 and 20. There is also a region of comparably high values centered at beam lag -7 and radial lag -22. It would be most difficult to develop an interpolation model to fit this situation since the true vector end might be in either of these two regions. While similar structures are quite common for other boxes, there are also many that are much more elliptical, the basic shape that Rinehart assumed for his interpolation model.

In addition to direction uncertainties, there must be magnitude uncertainties due to these resolution problems. A qualitative survey of the vectors in Figs. 4 and 9 reveals that the increase in time lag for the correlations results in a reduction in magnitudes, on average. One might consider a further increase of the time lag to allow for more motion between scans. However, one might expect some temporal decorrelation as seen by Rinehart [1979]. Fig. 11 is a graph of averaged maximum correlations versus temporal lag for 3 km x 2° and 6 km x 4° boxes. These are from April 10, 1979 data, times 1715 - 1723. The 66 and 132 s lags correspond to motions in Figs. 4 and 9. Correlations are quite high, ranging from 0.82 to 0.88 for the large boxes and from 0.85 to 0.92 for the small boxes. While the steady increase of the coefficient with increasing lag for the small box cannot be considered significant, the lack of decorrelation for both boxes leads one to expect that the quality of the motion fields would be fairly

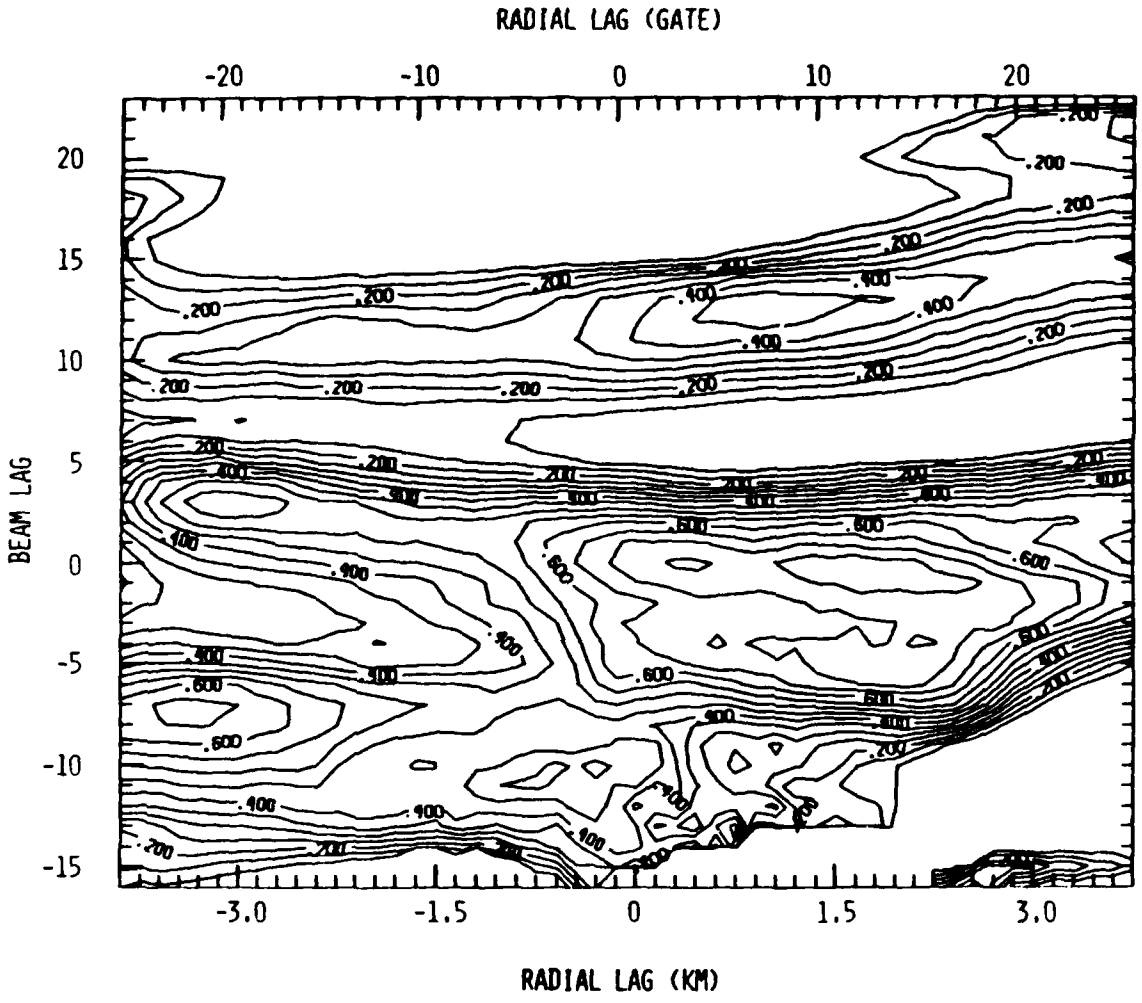

Fig. 10. Contours of Squares of Correlation Coefficients for a 6 km x 4° Box Lagged in Range and Azimuth

(Data are from June 22, 1976, scans 1625 and 1627. Contours corresponding to negative correlation coefficients are not shown. Each beam lag is ~0.6° and each radial lag is 150 m. All lags are measured relative to the center of the search area for V1 (see Fig. 1).)

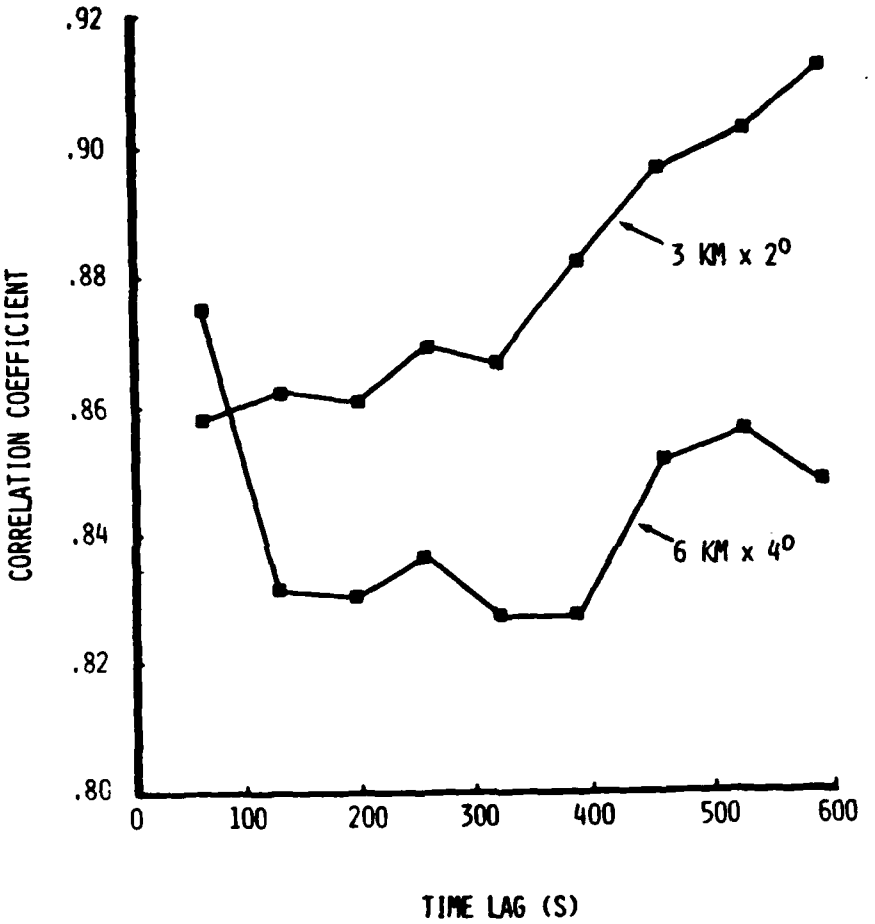

Fig. 11. Averaged Correlation Coefficient *vs.* Time Lag for Two Box Sizes, April 10, 1979, 1715-1723, 0.5° Elevation

good even at the longest lags. But other factors must be considered because, in fact, the number of randomly oriented vectors increased with longer lags. This may be a result of the lag times approaching the time scales of some of the features being correlated, i.e., the features are evolving significantly between scans, a propagational effect. This implies that the features are not unique.

In addition to the random vectors mentioned in the previous paragraph, there are other problems attributable to propagation. As noted before, the single radar motions at low levels are very much different from the airflow at those levels (Fig. 8). An explanation of these discrepancies may be found in the precipitation generator-trail theory first presented by Marshall [1953].[5] Basically, the theory states that precipitation patterns generated by and extending from convective cells will move with the speed and direction of the cell. The particles themselves are advected with the local wind, but this results only in the pattern being distorted vertically. Therefore pattern tracking below cloud base (which was done in our two cases) will result in motion fields characteristic not of the sub-cloud layer, but of some region within the active portion of the cloud. An attempt could be made to reduce the box size to find a scale of advection responsive to the local winds. However, data resolution is quite limited (1° in azimuth) and prohibits a significant reduction. Besides, the 3 km x 2° box produced only slight differences. This means that boundary layer wind estimates using correlation techniques are likely to be successful only in clear air cases where motions are decoupled from motions at higher levels. However, even there Smythe and Zrnic' [1983] noted some propagational effects in the correlation analyses of radial velocities in their clear air study, but not in the reflectivity analyses.

V. SUMMARY AND CONCLUSIONS

A correlation-pattern-recognition technique was applied to data from two intense thunderstorms to determine sub-cloud layer motions and perhaps obtain local winds. From this application it is clear that the technique

5. Marshall, J. S., 1953: Precipitation patterns and trajectories. J. Meteor., 10, 25-29.

does not detect air motions but instead it appears to track precipitation generators that are at heights above the analysis levels. It is likely that these motions are related to air motions in the more active layers of the storm but this relationship is not well-defined. The problem is likely to be aggravated when multiple scales of convection are present. For boundary layer wind estimations the technique should be used only when the boundary layer is effectively decoupled from the levels above it.

It was found that the quality of the motion fields derived from correlation techniques is very dependent upon the temporal and spatial resolution of the data. Considerable errors can result from the use of data with azimuthal resolution of ~1°, which is typical of weather radars. Increasing the time lag can reduce these errors, but longer lags introduce errors due to propagational effects.

Appendix - Horizontal Wind Algorithm

1. Algorithm Procedure

```
BEGIN ALGORITHM (HORIZONTAL WIND)
1.0 DO FOR ALL (SECTOR1'S)
  1.1 READ (8° of data from disk file containing previous scan data)
  1.2 READ (32° of data, centered azimuthally about SECTOR1, from disk file
      containing current scan data (SECTOR2'S)
  1.3 COMPUTE (TIME DIFFERENCE)
  1.4 Partition SECTOR1 into boxes 6 km in range (BOX1'S)
  1.5 DO FOR ALL (BOX1'S within a SECTOR1)
    1.5.1 Count the number of DOPPLER VELOCITIES in BOX1
    1.5.2 Determine the possible number of DOPPLER VELOCITIES in BOX1
    1.5.3 IF (Number of DOPPLER VELOCITIES in BOX1 is greater than 30% of the
            possible number of DOPPLER VELOCITIES in BOX1)
          THEN COMPUTE (MEAN DOPPLER VELOCITY IN BOX1)
               COMPUTE (STANDARD DEVIATION OF DOPPLER VELOCITIES IN BOX1)
               COMPUTE (RADIAL DISPLACEMENT)
               COMPUTE (TOLERANCE)
               Identify all 6 km x 8° boxes (BOX2'S) centered within ±
               (TOLERANCE) resolution volumes of (center of BOX1 + RADIAL
               DISPLACEMENT) and within the azimuthal limits of SECTOR2
               DO FOR ALL (BOX2'S)
                Determine the NUMBER OF VALUES OF REFLECTIVITY common to
                BOX1'S and BOX2'S
                Determine the possible number of common REFLECTIVITIES
                IF (Number of common REFLECTIVITIES is less than 30% of
                   possible number of common REFLECTIVITIES)
                 THEN COMPUTE (MEAN OF COMMON REFLECTIVITIES IN BOX1)
                      COMPUTE (COVARIANCE)
                      IF (COVARIANCE is greater than zero)
                        THEN COMPUTE (MEAN OF COMMON REFLECTIVITIES IN BOX2)
                             COMPUTE (SQUARE OF CORRELATION COEFFICIENT)
                      END IF
                END IF
               END DO
               IF (SQUARE OF CORRELATION COEFFICIENT is greater than e^-2)
                THEN COMPUTE (CARTESIAN COORDINATES TO CENTER OF BOX1)
                     Find BOX2 with maximum correlation coefficient and its
                     corresponding slant range and azimuth
                     COMPUTE (CARTESIAN COORDINATES TO CENTER OF BOX2 WITH
                             MAXIMUM CORRELATION COEFFICIENT)
                     COMPUTE (WIND SPEED)
                     IF (WIND SPEED is less than 40 m.s^-1)
                        THEN COMPUTE (WIND DIRECTION)
                             WRITE (SLANT RANGE TO CENTER OF BOX1)
                             WRITE (AZIMUTH ANGLE AT CENTER OF BOX1)
                             WRITE (WIND SPEED)
                             WRITE (WIND DIRECTION)
                             WRITE (SLANT RANGE TO CENTER OF BOX2)
                     END IF
               END IF
          END IF
    END DO
  END DO
```

Appendix - Horizontal Wind Algorithm (continued)

2.0 WRITE (Current time from TIMES)
END ALGORITHM (HORIZONTAL WIND)

2. COMPUTATION

2.1 NOTATION

V1	=	A Doppler velocity value in BOX1 in $m.s^{-1}$
TD	=	TIME DIFFERENCE in seconds
T_c	=	Current observation time in seconds
T_p	=	Previous observation time in seconds
$\overline{V1}$	=	MEAN DOPPLER VELOCITY IN BOX1 in $m.s^{-1}$
N1	=	The number of DOPPLER VELOCITIES in BOX1
i	=	An index for summations of DOPPLER VELOCITIES or REFLECTIVITIES
R1	=	A reflectivity value in BOX1 in dBZ
SD	=	STANDARD DEVIATION of velocities in BOX1
RD	=	RADIAL DISPLACEMENT in number of resolution volumes
dr	=	The length of a resolution volume in meters
TOL	=	TOLERANCE
R1	=	A reflectivity value in BOX1 in dBZ
$\overline{R1}$	=	MEAN OF COMMON REFLECTIVITIES IN BOX1 in dBZ
NN	=	The number of data points common to both BOX1 and BOX2
R2	=	A reflectivity value in BOX2 in dBZ
$\overline{R2}$	=	MEAN OF COMMON REFLECTIVITIES IN BOX2 in dBZ
COV	=	COVARIANCE
CC	=	CORRELATION COEFFICIENT
X1,Y1	=	CARTESIAN COORDINATES TO THE CENTER OF BOX1 in meters
SR_1	=	Slant range to the center of BOX1 in meters
θ_1	=	Azimuth angle to the center of BOX1 in degrees
X2,Y2	=	CARTESIAN COORDINATES TO CENTER OF BOX2 WITH MAXIMUM CORRELATION COEFFICIENT in meters
SR_2	=	Slant range to center of BOX2 with maximum correlation coefficient in meters
θ_2	=	Azimuth angle to center of the BOX2 with maximum correlation coefficient in degrees
WS	=	WIND SPEED in $m.s^{-1}$
WD	=	WIND DIRECTION in degrees (measured clockwise from North)
e	=	2.71828....

2.2 SYMBOLIC FORMULAS

COMPUTE (TIME DIFFERENCE)

$$TD = T_c - T_p$$

COMPUTE (MEAN DOPPLER VELOCITY IN BOX1)

$$\overline{V1} = \sum_{i=1}^{N1} V1_i / N1$$

Appendix - Horizontal Wind Algorithm (continued)

COMPUTE (STANDARD DEVIATION)

$$SD = \{[\sum_{i=1}^{N1} (V1_i - \overline{V1})^2]/N1\}^{1/2}$$

COMPUTE (RADIAL DISPLACEMENT)

$$RD = (\overline{V1})(TD/dr)$$

COMPUTE (TOLERANCE

$$TOL = (SD)(TD/dr)$$

COMPUTE (MEAN OF COMMON REFLECTIVITIES IN BOX1)

$$\overline{R1} = (\sum_{i=1}^{NN} R1_i)/NN$$

COMPUTE (COVARIANCE)

$$COV = [\sum_{i=1}^{NN} (R1_i - \overline{R1})(R2_i - \overline{R2})]/NN$$

COMPUTE (MEAN OF COMMON DOPPLER VELOCITIES IN BOX2)

$$\overline{R2} = (\sum_{i=1}^{NN} R2_i)/NN$$

COMPUTE (SQUARE OF CORRELATION COEFFICIENT)

$$(CC)^2 = [(NN)(COV)]^2/[\sum_{i=1}^{NN} (R1_i - \overline{R1})^2][\sum_{i=1}^{NN} (R2_i - \overline{R2})^2]$$

COMPUTE (CARTESIAN COORDINATES TO CENTER OF BOX1)

$$X1 = (SR_1)(\sin(\theta_1))$$

$$Y1 = (SR_1)(\cos(\theta_1))$$

COMPUTE (CARTESIAN COORDINATES TO CENTER OF BOX2 WITH MAXIMUM CORRELATION COEFFICIENT)

$$X2 = (SR_2)(\sin(\theta_2))$$

$$Y2 = (SR_2)(\cos(\theta_2))$$

COMPUTE (WIND SPEED)

$$WS = [(X2 - X2)^2 + (Y2 - Y1)^2]^{1/2}/TD$$

COMPUTE (WIND DIRECTION)

$$WD = \tan^{-1}\left(\frac{X2 - X1}{Y2 - Y1}\right)$$

END

FILMED

8-85

DTIC